International Scholarly Research Network
ISRN Mechanical Engineering
Volume 2011, Article ID 427976, 8 pages
doi:10.5402/2011/427976

Research Article

An Experimental Analysis of the Fluid Dynamic Efficiency of a Production Spark-Ignition Engine during the Intake and Exhaust Phase

Angelo Algieri

Mechanics Department, University of Calabria, Via P. Bucci, Cubo 46C, 87030 Arcavacata di Rende, Italy

Correspondence should be addressed to Angelo Algieri, a.algieri@unical.it

Received 30 January 2011; Accepted 16 March 2011

Academic Editors: K. Mekheimer, T. Y. Ng, and M. Vahdati

The present work aims at analyzing the fluid dynamic efficiency of a four-stroke spark-ignition engine. Specifically, a production four-cylinder internal combustion engine has been investigated during the intake and exhaust phase. The experimental characterization has been carried out at the steady flow rig adopting the dimensionless flow and discharge coefficients. The analysis has highlighted the great influence of the valve lift on the volumetric efficiency of the intake and exhaust system. Furthermore, the global investigation has demonstrated that the throttle angle has a significant influence on the head permeability during the induction phase. Particularly, the throttling process effect increases with the valve lift. Finally, the work has shown that all experimental data can be correlated by a single curve if an opportune dimensionless plot is adopted.

1. Introduction

A deep knowledge of the intake and exhaust processes is fundamental to design and optimize modern internal combustion engines (ICEs). The development of efficient intake and exhaust systems, in fact, plays a basic role both to reduce exhaust emissions and fuel consumptions and to improve the performances of actual engines [1–4].

To this purpose, different investigation tools, based on CFD codes [5–7] or experimental approaches [8–10], are available. In particular, to investigate the fundamentals of the intake and exhaust processes and to evaluate the fluid dynamic efficiency of engines, steady flow testing is a widely employed procedure in the ICE research community, owing to the relative simplicity, the proper simulation of the real phases, and the possibility of using real engine heads and components [11–13].

These analyses are based on dimensionless discharge and flow coefficients [14–17], that supply significant information on the fluid dynamic efficiency of engines during the intake and/or the exhaust processes. Furthermore, dimensionless coefficients provide practical advices to engine designers and tuners on the sizing and location of valves and ducts [13], and they represent a fundamental reference to develop and validate the CFD models that are adopted to simulate and optimize the modern engines [18].

The aim of the paper is the analysis and the characterization of the fluid dynamic behaviour of a production spark-ignition engine during the intake and the exhaust phase. A four-stroke internal combustion engine was examined at a steady flow rig in order to have detailed information on the global volumetric efficiency of the engine.

The influence of the valve lift and throttle valve opening on the head breathability was investigated adopting the discharge and flow coefficients. In fact, few quantitative studies on the effect of the throttling process on engine volumetric efficiency are available in the literature, in spite of the great influence of the throttle opening on the engine fluid dynamic efficiency. Finally, a dimensionless plot was used to correlate experimental data.

2. Methodology

The experimental analysis focused on a production spark-ignition engine. Figure 1 shows the engine head while

Figure 1: Engine head.

Table 1 lists the main engine characteristics. The fluid dynamic efficiency of the intake and exhaust apparatus was investigated at a steady flow rig, enabling air to be forced through the system by means of a blower. More details on the experimental apparatus are given in the literature [19–21]. During each measurement, the valve lift was fixed to a selected value. For the intake process, the dimensionless valve lift (L_v/D_v) was set in the 0.060–0.301 interval, whereas the corresponding range was 0.072–0.358 when the exhaust phase was characterised. Furthermore, in order to define the influence of the throttling process on the head permeability, the global analysis of the intake system was repeated at different throttle valve positions.

Measurements were carried out setting the pressure drop at $\Delta p = 10\,\text{kPa}$ for both the intake and the exhaust process. Specifically, for the intake phase the pressure drop corresponds to the difference between ambient and cylinder pressure. For the exhaust phase the pressure drop is measured as the difference between the cylinder and the ambient pressure.

Table 2 summarizes the analysed configurations and the measuring conditions.

Table 1: Main engine characteristics.

Engine	Four-stroke spark-ignition
Number of cylinders, N_c	4
Number of valves per cylinder, N_v	2
Stroke/Bore, L/B	1.167
Intake valve diameter/Bore, D_i/B	0.461
Exhaust valve diameter/Bore, D_e/B	0.387

Table 2: Measuring conditions.

Analysed system	Intake	Exhaust
Pressure drop, Δp	10 kPa	10 kPa
Dimensionless valve lift, L_v/D_v	$0.060 \div 0.301$	$0.072 \div 0.358$
Throttle angle, F	$30, 40, 50, 70, 90^\circ$	—

3. Discharge and Flow Coefficient

The discharge and flow coefficients were used to define the global fluid dynamic efficiency of the intake and exhaust system [1]. Specifically, the dimensionless coefficients are defined as the ratio of the measured mass flow rate $\dot{m}_{\text{meas}}$ to reference mass flow rate $\dot{m}_r$

$$C_f = \frac{\dot{m}_{\text{meas}}}{\dot{m}_r}. \tag{1}$$

If the flow is subsonic, the reference mass flow rate is given by

$$\dot{m}_r = A_{\text{ref}} \cdot \frac{p_0}{\sqrt{R \cdot T_0}} \cdot \left(\frac{p_T}{p_0}\right)^{1/\gamma} \cdot \left\{\frac{2 \cdot \gamma}{\gamma - 1} \cdot \left[1 - \left(\frac{p_T}{p_0}\right)^{(\gamma-1)/\gamma}\right]\right\}^{1/2}, \tag{2}$$

while, if the flow is choked, the mass flow is formalized as follows:

$$\dot{m}_r = A_{\text{ref}} \cdot \frac{p_0}{\sqrt{R \cdot T_0}} \cdot \gamma^{1/2} \left(\frac{2}{\gamma + 1}\right)^{(\gamma+1)/[2\cdot(\gamma-1)]}, \tag{3}$$

where p_0 is the intake system pressure when the intake phase is analysed (or the cylinder pressure when the exhaust phase is considered), p_T is the cylinder pressure when the intake phase is investigated (or the exhaust system pressure when the exhaust phase is analysed), T_0 is the intake system temperature when the intake phase is considered (or the cylinder temperature when the exhaust phase is investigated), and A_{ref} is the reference area.

The difference between the discharge and flow coefficient lies in the definition of the reference area A_{ref} [9]. For the discharge coefficient, this area is the valve curtain area and, therefore, it is a linear function of valve lift L_v

$$A_{\text{ref}} = \pi \cdot D_v \cdot L_v. \tag{4}$$

For the flow coefficient, the reference area is given by the valve outer seat area:

$$A_{\text{ref}} = \frac{\pi \cdot D_v^2}{4}. \tag{5}$$

Furthermore, absolute flow coefficients C_{abs} were defined to characterize the intake and the exhaust system efficiency independently of the valve lift [22]

$$C_{\text{abs}} = \frac{\phi_{\text{Am}}}{\phi_{\text{Ad}}}, \tag{6}$$

where ϕ_{Ad} represents the dimensionless theoretical flow rate downstream of the valve, based on the isentropic flow condition

$$\phi_{\text{Ad}} = \sqrt{\frac{2}{\gamma - 1} \cdot \left[\left(\frac{p_T}{p_0}\right)^{2/\gamma} - \left(\frac{p_T}{p_0}\right)^{(\gamma+1)/\gamma}\right]}, \tag{7}$$

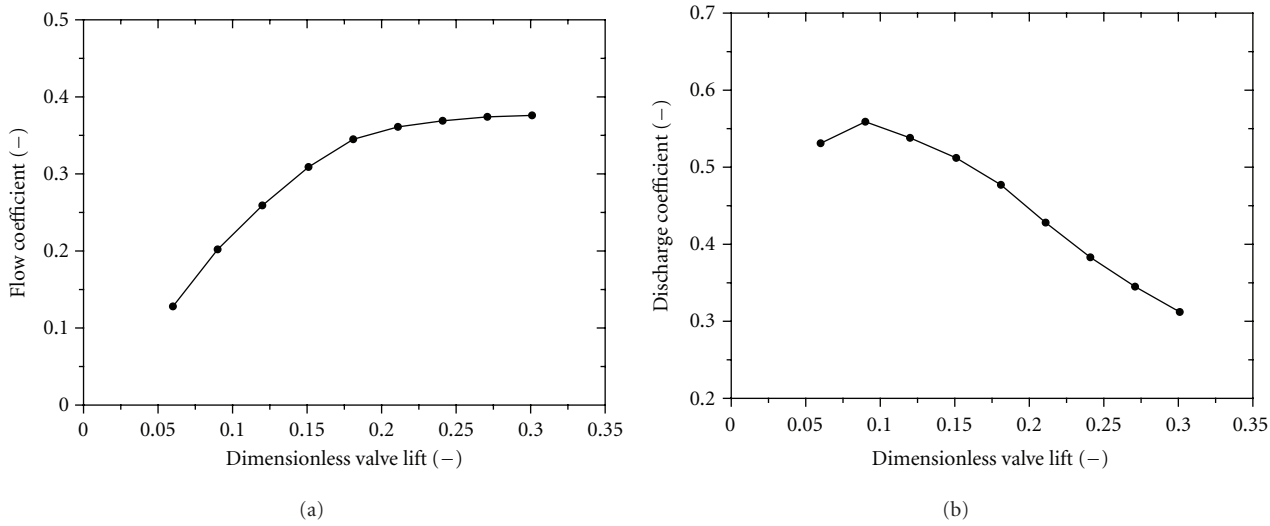

(a) (b)

Figure 2: Influence of valve lift on flow (a) and discharge (b) coefficients. Intake phase—Wide open throttle (WOT) configuration.

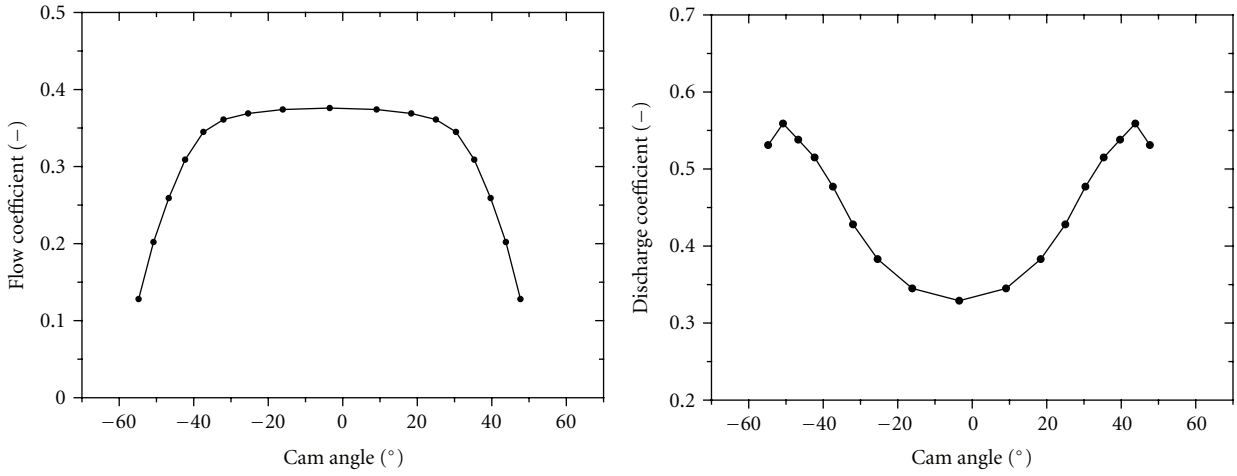

(a) (b)

Figure 3: Influence of cam angle on flow (a) and discharge (b) coefficients. Intake phase—Wide open throttle (WOT) configuration.

while ϕ_{Am} is the dimensionless actual flow rate, averaged over the dimensionless valve lift

$$\phi_{\mathrm{Am}} = \frac{\int_0^{(L_v/D_v)_{\max}} \dot{m}_{\mathrm{meas}}/(A_{\mathrm{ref}} \cdot \rho_0 \cdot a_0) \cdot d(L_v/D_v)}{(L_v/D_v)_{\max}}, \quad (8)$$

where ρ_0 is the air density and a_0 is the sound speed.

Moreover, mean flow coefficients were calculated in line with Li et al. [23]

$$C_{f\,\mathrm{Mean}} = \frac{1}{\alpha_2 - \alpha_1} \cdot \int_{\alpha_1}^{\alpha_2} C_f \cdot d\alpha, \quad (9)$$

where α is the cam angle, 1 refers to the minimum cam angle, and 2 refers to the maximum cam angle.

The overall uncertainty of dimensionless flow coefficients and absolute flow coefficients was always lower than 3%, and it decreased with valve lift and throttle angle.

4. Results

Figure 2 shows the fluid dynamic efficiency of the intake system in terms of flow and discharge coefficients as a function of the dimensionless valve lift (L_v/D_v). The figure refers to the wide-open throttle (WOT) configuration. A progressive raise in the flow coefficient is observed when the valve lift increases, while decreasing values of the discharge coefficient are registered for $L_v/D_v > 0.090$. Data reflect the continuous upsurge in the mass flow rate entering the combustion chamber. A plateau is reached for $L_v/D_v > 0.241$, and there are negligible effects on the head breathability owing to the dimensions of the intake port and the valve stem that define the minimum flow area at high valve lifts. Figure 2 reveals also the presence of different regions, characterized by decreasing slopes in the flow coefficient's curve, which corresponds to different flow regimes. This finding is in line

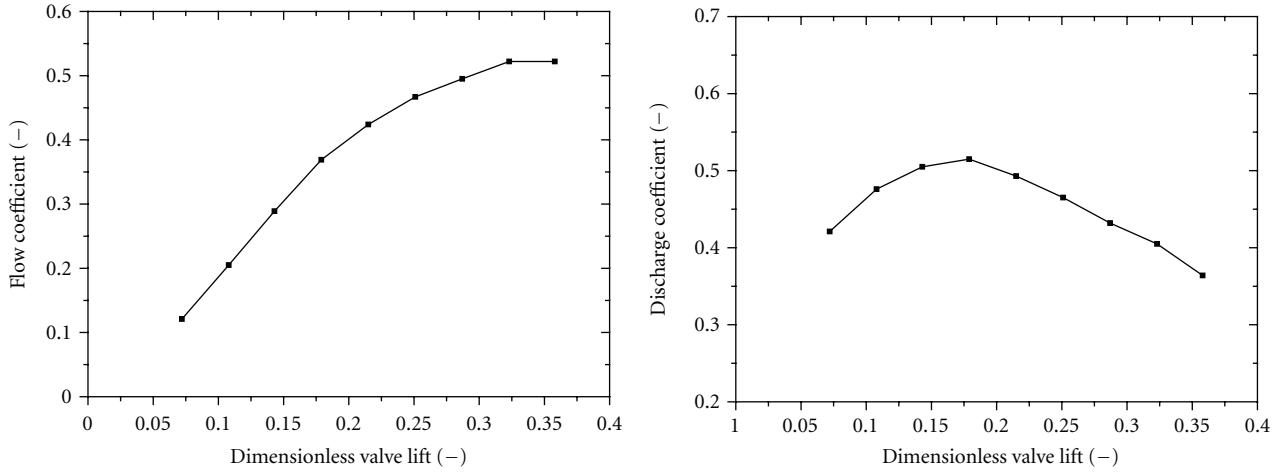

(a) (b)

Figure 4: Influence of valve lift on flow (a) and discharge (b) coefficient. Exhaust phase.

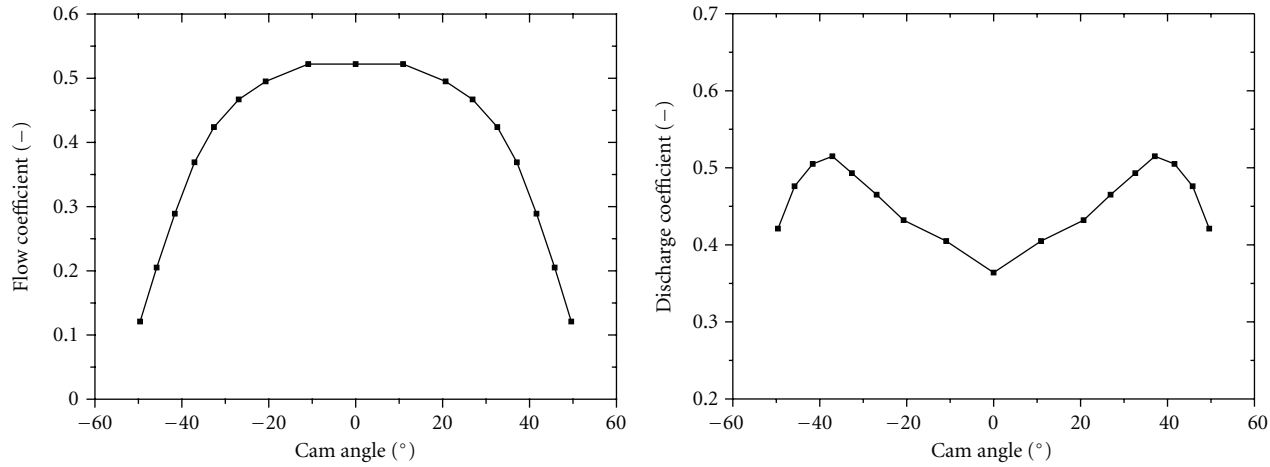

(a) (b)

Figure 5: Influence of cam angle on flow (a) and discharge (b) coefficient. Exhaust phase.

with the literature [1, 24]. Specifically, for low valve lift, the flow remains attached to the valve seat and head due to the high viscous phenomena. When the curtain area increases, it is possible to observe a flow separation, firstly, at the valve head and, successively, at the valve seat.

Figure 3 shows the two dimensionless coefficients versus the cam angle, while Table 3 resumes the absolute dimensionless coefficients. It is evident that the flow coefficient, and in turn the mass flow rate, maintains values larger than 80% of the maximum level for about 80° of the cam angle, whereas the absolute coefficients reach the 77.4% and 83.9% of the maximum flow and discharge coefficient, respectively.

At the same time, the fluid dynamic behaviour of the exhaust system has been evaluated. To this purpose, the flow from the cylinder through the exhaust valve has been characterized (Figure 4). Specifically, the same pressure drop ($\Delta p = 10$ kPa), adopted during the fluid dynamic characterization of the intake apparatus, has been imposed between the combustion chamber and the exhaust system.

Table 3: Absolute and mean flow coefficients for the intake system-WOT configuration.

Analysed system	Intake
Throttle angle, F	90°
Absolute flow coefficient, $C_{f\,\mathrm{Abs}}$	0.291
Absolute discharge coefficient, $C_{d\,\mathrm{Abs}}$	0.469
Mean flow coefficient, $C_{f\,\mathrm{Mean}}$	0.330
Mean discharge coefficient, $C_{d\,\mathrm{Mean}}$	0.427
Maximum flow coefficient, $C_{f\,\mathrm{Max}}$	0.376
Maximum discharge coefficient, $C_{d\,\mathrm{Max}}$	0.559

The figure depicts a continuous increase in the flow coefficient when the valve lift increases, because of the progressive raise in the exhaust mass flow rate. A plateau is found for $L_v/D_v > 0.323$ and negligible effects on the head breathability at high valve lifts are visible. Here, the

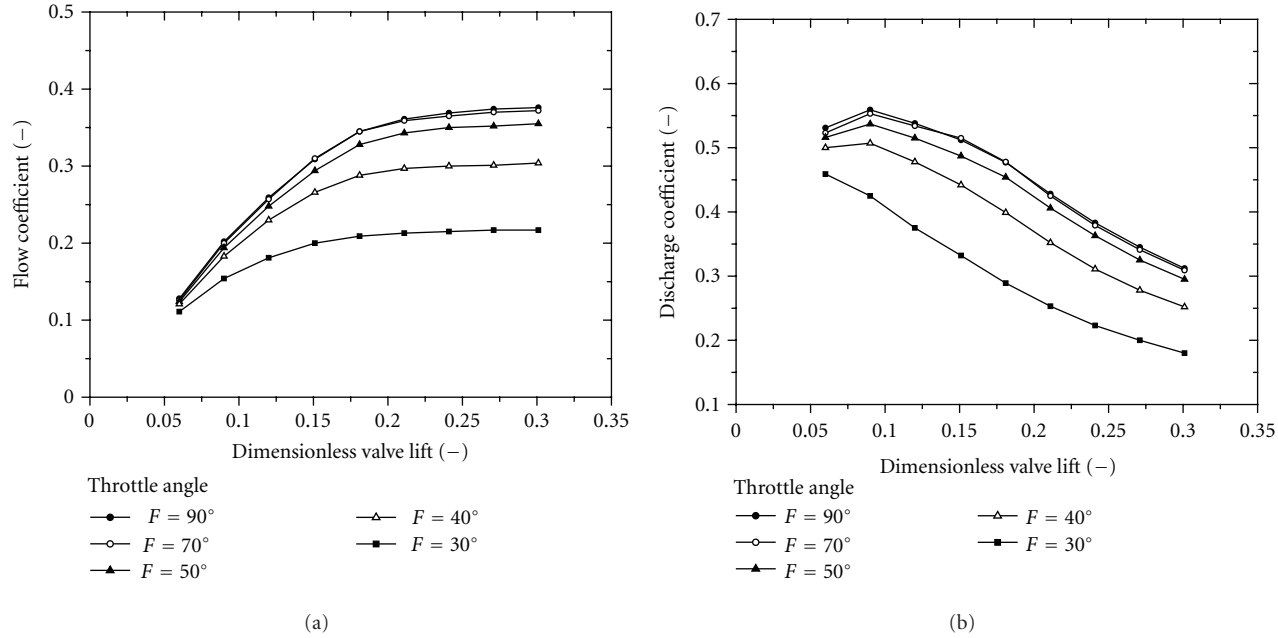

Figure 6: Influence of throttle angle on head permeability in terms of dimensionless flow (a) and discharge (b) coefficient. Intake phase.

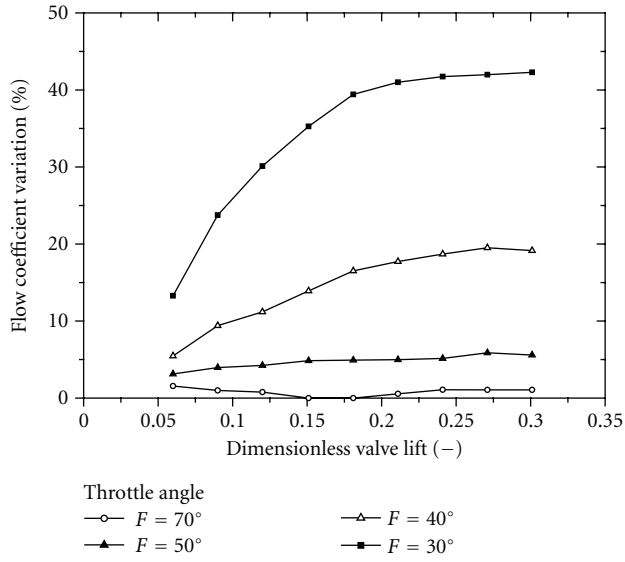

Figure 7: Percentage difference in dimensionless flow coefficients between WOT and throttled configurations. Intake phase.

dimensions of the exhaust port and the valve stem define the minimum flow area, as already observed for the intake system. Moreover, the analysis reveals that the discharge coefficient presents the maximum value at $L_v/D_v = 0.179$. At higher lifts, the flow separation both at the valve head and seat reduces significantly the effective flow area and, as a consequence, the discharge coefficient drops in line with the literature results [1].

The two dimensionless coefficients versus the cam angle for the exhaust system are plotted in Figure 5, whereas

Table 4: Absolute and mean flow coefficients for the exhaust system.

Analysed system	Exhaust
Absolute flow coefficient, $C_{f\,\mathrm{Abs}}$	0.359
Absolute discharge coefficient, $C_{d\,\mathrm{Abs}}$	0.458
Mean flow coefficient, $C_{f\,\mathrm{Mean}}$	0.426
Mean discharge coefficient, $C_{d\,\mathrm{Mean}}$	0.448
Maximum flow coefficient, $C_{f\,\mathrm{Max}}$	0.522
Maximum discharge coefficient, $C_{d\,\mathrm{Max}}$	0.515

Table 4 outlines the absolute coefficients, that correspond to the 68.8% and 88.9% of the maximum flow and discharge coefficients, respectively. The comparison between the intake (Figure 3) and the exhaust (Figure 5) system put in evidence that the variation in the flow coefficient with the cam angle is more rapid when the exhaust process is analysed.

In order to investigate the influence of throttling process on the intake system breathability, the global analysis was also performed at several throttle angles (Figure 6). Table 2 illustrates the analysed configurations.

Experimental data put in evidence similar behaviours for the different throttle positions and the presence of the three flow regimes. It is possible to observe that the "transition" from a flow condition to another one is reached at lower valve lift values when the flow is throttled. As an example, the transition phenomena for the wide-open throttle configuration ($F = 90°$) occur at the valve lift $L_v/D_v = 0.120$ and $L_v/D_v = 0.241$, while for $F = 30°$, they develop at $L_v/D_v = 0.090$ and $L_v/D_v = 0.231$, respectively.

In addition, the plot illustrates the noticeable influence of the throttle valve opening on the volumetric efficiency of the intake system. As expected, a progressive increase in the head

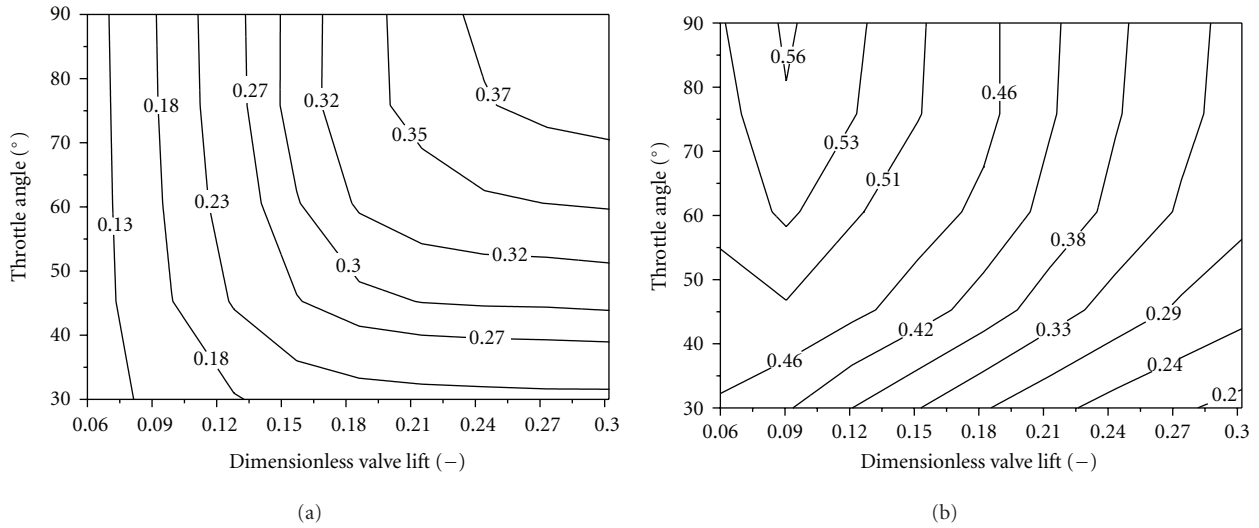

Figure 8: Dimensionless flow (a) and discharge (b) coefficients contour plot. Intake phase.

Table 5: Influence of the throttle angle on the absolute and mean flow coefficients. Intake system.

Throttle angle, F	90°	70°	50°	40°	30°
Absolute flow coefficient, $C_{f\,\mathrm{Abs}}$	0.291	0.289	0.277	0.246	0.185
Absolute discharge coefficient, $C_{d\,\mathrm{Abs}}$	0.469	0.466	0.448	0.407	0.321
Mean flow coefficient, $C_{f\,\mathrm{Mean}}$	0.330	0.328	0.313	0.253	0.202
Mean discharge coefficient, $C_{d\,\mathrm{Mean}}$	0.427	0.424	0.406	0.373	0.272
Maximum flow coefficient, $C_{f\,\mathrm{Max}}$	0.376	0.372	0.355	0.304	0.217
Maximum discharge coefficient, $C_{d\,\mathrm{Max}}$	0.559	0.553	0.537	0.507	0.459

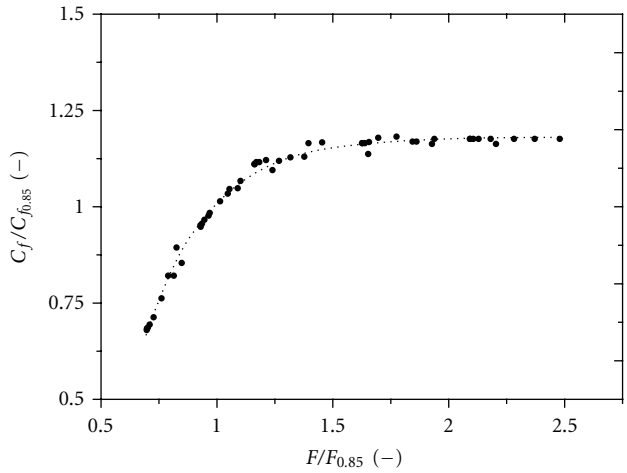

Figure 9: Universal trend in the dimensionless flow coefficients. Intake phase.

permeability is observed when the throttle angle upsurges. However, this effect tends to reduce significantly with the throttle angle and there are small effects on the fluid dynamic efficiency of the intake system when $F > 70°$. Specifically, the percentage variations between the WOT configuration (assumed as a reference) and the throttled configurations are reported in Figure 7. The analysis highlights that the differences raise with the valve lift and by throttling the flow. Specifically, the values are always lower than 1.6% when the throttle angle passes from $F = 70°$ to $F = 90°$. Conversely, by moving from $F = 30°$ to the WOT configuration, the relative growth in the fluid dynamic efficiency is always higher than 13.3% and it is larger than 41.0% for $L_v/D_v > 0.211$.

This trend is also visible in Table 5, which presents the absolute and the mean coefficients (calculated according to (6) and (9), resp.) for the five throttle angles. Former experimental results, referring to the intake system, are resumed in Figure 8.

Finally, all the experimental data were correlated by adopting a new dimensionless plot, defined in a former work [25]. The previous research activity, carried out on a high performance four-stroke motorcycle engine, put in evidence that all the experimental data tend to distribute along the same curve if they are plotted as

$$\frac{C_f}{C_{f\,0.85}} = f\left(\frac{F}{F_{0.85}}\right), \tag{10}$$

where $C_{f\,0.85}$ is the dimensionless coefficient corresponding to 85% of the maximum flow coefficient, and $F_{0.85}$ is the throttle angle where the dimensionless coefficient C_f is equal to 85% of the maximum value.

Figure 9 confirms the presence of a universal trend in the flow coefficient also for the actual engine. In particular, the

data are well approximated by an exponential curve, whose equation is

$$\frac{C_f}{C_{f\,0.85}} = a + b \cdot e^{-c\cdot(F/F_{0.85})}, \tag{11}$$

where the values of the three constants are $a = 1.1811$, $b = -6.5092$, and $c = 3.6459$.

The result is very useful because it guarantees a drastic reduction in the measurements that have to be done to characterize the fluid dynamic efficiency of the engine intake system. As a consequence, time and costs of the investigations are decreased. At the same time, plotting the experimental data in the suggested form facilitates the check during the measuring phase. Obviously, further analysis should be performed to verify the extensibility of the previous law to other engines.

5. Conclusions

An experimental investigation was performed to analyse the fluid dynamic efficiency of a production internal combustion engine during the intake and the exhaust phase. Specifically, the attention was focused on a multicylinder spark-ignition engine.

Measurements were carried out at a steady flow rig, and discharge and flow coefficients were used to characterise the global engine breathability.

The global analysis has revealed the significant influence of the valve lift on the fluid dynamic efficiency of the intake and exhaust system. Different flow regimes have been registered, and flow separation phenomena at the valve head and seat have been observed at high valve lifts, in line with the literature results.

Furthermore, the investigation has shown the large effect produced by the throttle angle on the engine volumetric efficiency. A progressive increase in the head permeability was observed with the throttle angle opening. However, this effect became negligible when the throttle opening was larger than 70°. Moreover, the experimental characterisation has put in evidence that the transition phenomena from a flow condition to another one is reached at lower valve lifts when the flow is throttled.

Finally, the global analysis has demonstrated that a unique trend in the fluid dynamic efficiency of the intake system exists if an opportune dimensionless plot is adopted.

References

[1] J. B. Heywood, *Internal Combustion Engine Fundamentals*, McGraw Hill, New York, NY, USA, 1998.

[2] I. G. Hwang, C.-L. Myung, S. Park, C.-B. In, and G. K. Yeo, "Theoretical and experimental flow analysis of exhaust manifolds for PZEV," SAE paper 2007-01-3444, 2007.

[3] W. Zhijun and H. Zhen, "In-cylinder swirl formation process in a four-valve diesel engine," *Experiments in Fluids*, vol. 31, no. 5, pp. 467–473, 2001.

[4] J. M. Desantes, J. Galindo, C. Guardiola, and V. Dolz, "Air mass flow estimation in turbocharged diesel engines from in-cylinder pressure measurement," *Experimental Thermal and Fluid Science*, vol. 34, no. 1, pp. 37–47, 2010.

[5] H. Jasak, J. Y. Luo, B. Kaludercic et al., "Rapid CFD simulation of internal combustion engines," SAE paper 1999-01-1185, 1999.

[6] G. M. Bianchi and S. Fontanesi, "On the applications of low-Reynolds cubic k-ε turbulence models in 3D simulations of ICE intake flows," SAE paper 2003-01-0003, 2003.

[7] C. R. Siqueira, M. P. Kessler, R. Rampazzo, and D. A. Cardoso, "Three-dimensional numerical analysis of flow inside exhaust manifolds," SAE paper 2006-01-2623, 2006.

[8] K. Haga, I. Hidayah, Y. Shinozaki et al., "Flow visualization in exhaust manifold for automobile engine," SAE paper 2009-28-0005, 2009.

[9] H. Xu, "Some critical technical issues on the steady flow testing of cylinder heads," SAE paper 2001-01-13, 2001.

[10] K. Y. Kang and J. H. Baek, "LDV measurement and analysis of tumble formation and decay in a four-valve engine," *Experimental Thermal and Fluid Science*, vol. 11, no. 2, pp. 181–189, 1995.

[11] G. P. Blair, D. McBurney, P. McDonald, P. McKernan, and R. Fleck, "Some fundamental aspects of the discharge coefficients of cylinder porting and ducting restrictions," SAE paper 980764, 1998.

[12] G. P. Blair and F. M. M. Drouin, "Relationship between discharge coefficients and accuracy of engine simulation," SAE paper 962527, 1996.

[13] S. V. Bohac and K. Landfahrer, "Effects of pulsating flow on exhaust port flow coefficients," SAE paper 1999-01-0214, 1999.

[14] A. R. Ismail, Semin, and R. A. Bakar, "Valve flow discharge coefficient investigation for intake and exhaust port of four stroke diesel engines," *Journal of Engineering and Applied Sciences*, vol. 2, no. 12, pp. 1807–1811, 2007.

[15] J.-W. Son, S. Lee, B. Han, and W. Kim, "A correlation between re-defined design parameters and flow coefficients of SI engine intake ports," SAE paper 2004-01-0998, 2004.

[16] B. J. Fleck, R. Fleck, R. J. Kee, and D. J. Thornhill, "The evaluation of discharge coefficients in the cylinders of high performance two-stroke engines," SAE paper 2003-32-0029, 2003.

[17] A. R. Ismail, R. A. Bakar, and Semin, "Engine power calculation using air flow through engine from flowbench test flow of four stroke direct injection diesel engines," *Journal of Engineering and Applied Sciences*, vol. 2, no. 12, pp. 1812–1817, 2007.

[18] H. Jasak, J. Y. Luo, B. Kaludercic et al., "Rapid CFD simulation of internal combustion engines," SAE paper 1999-01-1185, 1999.

[19] A. Algieri, S. Bova, and C. De Bartolo, "Experimental and numerical investigation on the effects of the seeding properties on IDA measurements," *Journal of Fluids Engineering*, vol. 127, no. 3, pp. 514–522, 2005.

[20] A. Algieri, S. Bova, C. De Bartolo, and A. Nigro, "Numerical and experimental analysis of the intake flow in a high performance four-stroke motorcycle engine: influence of the two-equation turbulence models," *Journal of Engineering for Gas Turbines and Power*, vol. 129, no. 4, pp. 1095–1105, 2007.

[21] A. Algieri, C. De Bartolo, D. Mendicino, and A. Nigro, "Numerical and experimental investigation of the intake system of a high performance internal combustion engine," in

Proceedings of FISITA World Automotive Congress, Budapest, Hungary, May-June 2010.

[22] M. Auriemma, G. Caputo, F. E. Corcione, G. Valentino, and G. Riganti, "Fluid-dynamic analysis of the intake system for a HDDI diesel engine by STAR-CD code and LDA technique," SAE paper 2003-01-0002, 2003.

[23] Y. Li, H. Zhao, B. Leach, T. Ma, and N. Ladommatos, "Optimisation of in-cylinder flow for fuel stratification in a three-valve twin-spark-plug SI engine," SAE paper 2003-01-0635, 2003.

[24] M. Weclas, A. Melling, and F. Durst, "Unsteady intake valve gap flow," SAE paper 952477, 1995.

[25] A. Algieri, S. Bova, and C. De Bartolo, "Influence of valve lift and throttle angle on intake flow in a high-performance four-stroke motorcycle engine," *Journal of Engineering for Gas Turbines and Power*, vol. 128, no. 4, pp. 934–941, 2006.